



## Study of strain relaxation in CdSe/ZnSe nanostructures

L. Borkovska<sup>a</sup>, R. Beyer<sup>b</sup>, O. Gudymenko<sup>a</sup>, V. Kladko<sup>a</sup>, N. Korsunskaya<sup>a</sup>,  
T. Kryshchak<sup>c,\*</sup>, Yu. Sadofyev<sup>d</sup>, Ye. Venger<sup>a</sup>, J. Weber<sup>b</sup>

<sup>a</sup>*Institute of Semiconductor Physics NASU, Pr. Nauky, 45, Kyiv, 03028, Ukraine*

<sup>b</sup>*Institute of Applied Physics TU Dresden, D-01062, Germany*

<sup>c</sup>*Department of Material Sciences, ESFM-IPN, Av. IPN, Ed.9 U.P.A.L.M., 07738 Mexico D.F., Mexico*

<sup>d</sup>*Lebedev Physical Institute RAS, Leninskii pr.53, Moscow 117924, Russian Federation*

Available online 19 December 2004

### Abstract

Strain relaxation in CdSe/ZnSe self-assembled quantum dot (QD) and CdZnSe/ZnSe quantum well (QW) structures have been investigated by the photoluminescence (PL) and high-resolution X-ray diffraction methods. The PL spectra of the QW structures revealed that splitting of free exciton line in ZnSe cap layer is influenced significantly by Cd content in QWs that allows to obtain information about strain in quantum-confinement structures. It is shown that information about strain relaxation mechanism and interdiffusion processes can be obtained from the analysis of the PL spectra of free and bound excitons. It is found that strain relaxation in the QD structures occurs mainly via QD formation in spite of generation of extended defects. Significant doping of ZnSe cap layer with Cd is found both in the QW and QD structures. The data obtained from the simulations of X-ray diffraction profiles qualitatively proved the results obtained from the analysis of ZnSe excitonic spectra. The reasons of quantitative discrepancy are discussed.

© 2004 Elsevier B.V. All rights reserved.

PACS: 78.6.6.Hf; 61.10.Kw; 68.65.+g

Keywords: A1. Nanostructures; A1. Stresses; B2. Semiconducting II–VI materials

### 1. Introduction

In the last decade, MBE-grown CdSe/ZnSe heterostructures attracted great attention due to their potential application in high-efficiency visible

light-emitting devices. However, blue–green lasers based on CdZnSe quantum wells (QWs) still have insufficient lifetime [1]. Use of the layers containing CdSe self-assembled quantum dots (QDs) as an active media enabled to decrease the threshold power density of the laser as well as to increase its differential gain and stability [2]. The latter was supposed to be due to lower strains in the device active region [2]. Therefore, investigation of the

\*Corresponding author. Tel.: +52 55 57296000x55321; fax: +52 55 55862825.

E-mail address: [tkrysh@esfm.ipn.mx](mailto:tkrysh@esfm.ipn.mx) (T. Kryshchak).

peculiarities of strain relaxation in CdSe/ZnSe QD structures is of interest. Besides, CdSe/ZnSe QD organization was found to be quite complicated and accompanied by Cd/Zn interdiffusion as well as defect generation [3,4]. This necessitates monitoring of the last two processes.

X-ray diffraction methods are usually used for control of strain and structural quality (extended and point defects, interdiffusion) of single crystals and heterostructures. However, for multilayer structures it is difficult to separate the influence of different structure parameters of the layers of the same compounds on the profiles of X-ray rocking curves. In this case additional methods of investigations are desirable to use. One of such methods is the low-temperature photoluminescence (PL). In this method strains can be evaluated from splitting of exciton line, while point and extended defects can be identified from specific bands. Besides, as it will be shown below, the information about interdiffusion can be obtained from the PL spectra. But identification of defect-related bands in the PL spectra from quantum-confined layers is difficult. Therefore, we studied strain relaxation in CdZnSe/ZnSe nanostructures by high-resolution X-ray diffraction (HRXRD) and PL spectroscopy of ZnSe cap layers.

## 2. Experimental procedure

Two types of CdSe/ZnSe nanostructures MBE-grown on GaAs substrates were investigated: (i) the structures containing single  $\text{Cd}_x\text{Zn}_{1-x}\text{Se}$  QW; (ii) the structures containing single CdSe QD layer. QW thickness was 6 nm and the cadmium molar fraction  $x$  was 0.23, 0.35 and 0.43 in different samples. Nominal thickness of CdSe layer was 3.5 or 5 monolayers (ML).

The QW and QD structures were grown at VI/II group beam pressure ratio 2:1 and 4:1 and temperature 280–320 and 230–280 °C, respectively. Usually to stimulate the process of QD formation the growth interruption [5] or thermal annealing step [6] are used. In our QD structures thermal annealing at 340 °C was applied.

The QW samples were grown on 1300 nm ZnSe buffer layer and capped by 250 nm ZnSe layer. The

QD samples were grown on 250 nm ZnSe buffer layer and capped by 150 nm ZnSe layer. ZnSe epilayers (ELs) of 1500 and 200 nm thickness MBE-grown on GaAs substrates were also investigated for comparison.

The stationary PL spectra were measured in the temperature range  $T = 4.2\text{--}300\text{ K}$  under excitation by 325 nm line of HeCd laser. For time-resolved PL measurements a frequency doubled titanium sapphire laser, mode locked at 438 nm, was used. The light was detected by a Hamamatsu streak camera with a multichannel plate-enhanced CCD (HPD-TA). The HRXRD measurements were carried out using the X-ray diffractometer Philips MRD with a  $4 \times \text{Ge (220)}$  monochromator and Cu anode.

## 3. Experimental results

Fig. 1 shows 4.2 K PL spectra of two  $\text{Cd}_x\text{Zn}_{1-x}\text{Se}/\text{ZnSe}$  QW structures with  $x$  equal to 0.23 and 0.43 and two CdSe/ZnSe QD structures with the nominal thickness of CdSe insert of 3.5 and 5 ML.

The PL spectra of the QW samples (Fig. 1, solid lines) are dominated by emission band  $I_{\text{QW}}$  caused by radiative recombination of excitons in the

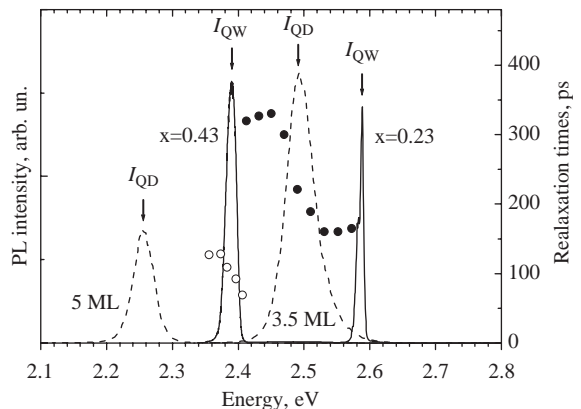


Fig. 1. PL spectra of two  $\text{Cd}_x\text{Zn}_{1-x}\text{Se}/\text{ZnSe}$  heterostructures with single QW of 6 nm thickness and with  $x = 0.23$  and 0.43 and two CdSe/ZnSe QD structures with 3.5 and 5 ML CdSe inserts,  $T = 4.2\text{ K}$ ,  $\lambda_{\text{exc}} = 325\text{ nm}$ . PL decay times are plotted as a function of the detection energy for the QW (open circles) and QD (solid circles) samples.

QWs. These excitons are either bound on defects or localised by potential fluctuations in the QW [7,8]. In the PL spectra of the QD samples (Fig. 1, dashed lines)  $I_{QD}$  band caused by radiative recombination of excitons in CdZnSe QDs dominates. The half-width of the  $I_{QD}$  band ( $\sim 40$  meV) is much larger than half-width of the  $I_{QW}$  band (9.7–15 meV in different samples) that is usually explained by dispersion of QDs both in composition and in size [5,6,9].

Different nature of the excitonic luminescence in the samples of two types is proved by time-resolved PL measurements. The PL decays measured at different detection energies within the  $I_{QW}$  and  $I_{QD}$  bands are almost monoexponential that enables to determine the PL decay times. The PL decay times are presented in Fig. 1 for QW structure with  $x = 0.43$  and 3.5 ML QD sample. The QW PL decay times within the  $I_{QW}$  bands are 90–130 ps (Fig. 1). These values are typical for QW with potential fluctuations [5,6]. The PL decay times for the QD samples are found to be twice as much as decay times in the QW samples due to stronger exciton localization in QDs [5,6].

The latter is proved by the temperature dependencies of the shift of  $I_{QD}$  and  $I_{QW}$  band positions, which are presented in Fig. 2. For both QW and QD samples the shift of the PL band position slower than CdSe and ZnSe band gap shrinkage is observed. This shift is attributed to thermal excitation of excitons from the deepest potential

minima to higher energy states [10]. In the QD sample this shift occurs at higher temperatures ( $T \sim 100$  K) than that in the QW sample ( $T \sim 40$  K). This indicates more strong exciton localization in the QDs compared to that in the QW potential fluctuations. Besides for  $T < 100$  K the  $I_{QD}$  band position shifts to the low-energy region stronger than CdSe and ZnSe band gap shrunk. This is the characteristic feature of the QD structures and is ascribed to thermal transfer of excitons from shallower to deeper potential minima in QD ensemble [10].

The luminescence characteristics mentioned above are typical for CdSe/ZnSe QW and QD structures obtained by MBE method.

In the PL spectra of both QW and QD samples weak emission lines caused by radiative recombination of excitons in ZnSe layers are observed. Taking into account ZnSe band-to-band absorption coefficient ( $\sim 10^5 \text{ cm}^{-1}$ ) and decrease of diffusion length of carriers in ZnSe due to effective capture and recombination of carriers in QWs we can think that ZnSe excitonic emission is excited mainly in the cap layer. This part of the PL spectra of the QW and QD structures is shown in Figs. 3a and b, respectively. In the same figures, the edge emissions of ZnSe ELs of 1500 and 200 nm thickness are also presented.

In all spectra presented in Fig. 3a the free exciton band splitted by the deformation potential on heavy-hole  $X_{hh}$  and light-hole components  $X_{lh}$ , the peaks of excitons bound to neutral donors  $\text{Ga}_{Zn}$  ( $I_2$ ) and neutral acceptors  $\text{V}_{Zn}$  ( $I_1$ ) [11] as well as  $I_V^0$  line related to exciton bound to threading dislocations [12] are observed.

The value of relative deformations  $\varepsilon$  in ZnSe layers was estimated from the energy difference between  $X_{hh}$  and  $X_{lh}$  components that is expressed by

$$X_{hh} - X_{lh} = -2b\varepsilon(C_{11} + 2C_{12})/C_{11}, \quad (1)$$

where  $b = -1.2$  eV is the shear deformation potential,  $C_{11} = 8.59 \times 10^{10}$  and  $C_{12} = 5.06 \times 10^{10} \text{ N m}^{-2}$  are the elastic stiffness constants for ZnSe [11].

The estimations show tensile relative deformations  $\varepsilon = 0.66 \times 10^{-3}$  in 1500 nm ZnSe EL. It means that compressive strain in ZnSe caused by lattice mismatch of ZnSe and GaAs significantly

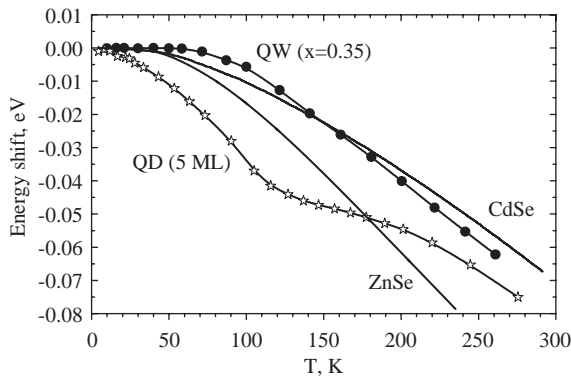


Fig. 2. Energy shift vs. temperature of the  $I_{QD}$  and  $I_{QW}$  band positions for 3.5 ML QD sample and QW structure with  $x = 0.35$ , respectively. The temperature dependencies of the ZnSe and CdSe band gap shift are plotted for comparison.

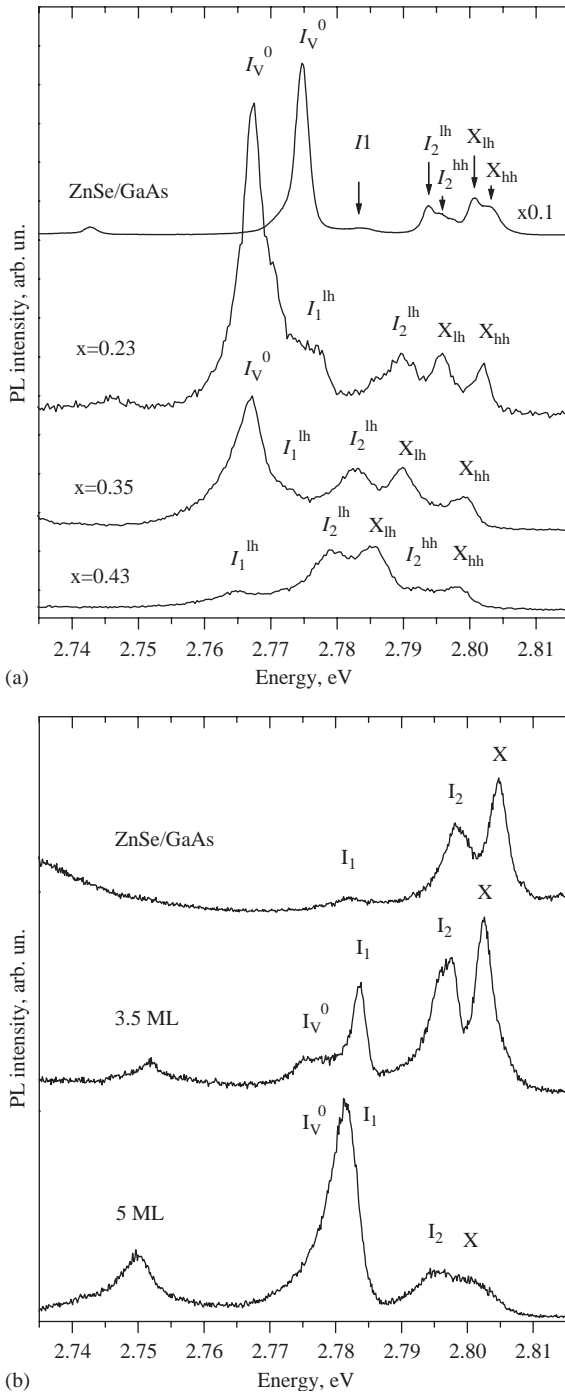


Fig. 3. Excitonic spectra of the ZnSe cap layer of the QW samples (a) with  $x = 0.23$ ,  $0.35$  and  $0.43$  and QD structures (b) with 3.5 and 5 ML CdSe inserts,  $T = 4.2$  K,  $\lambda_{exc} = 325$  nm. Edge emissions of ZnSe ELs of 1500 nm (a) and 200 nm (b) thickness are plotted for comparison.

relaxes at growth temperature that is proved by high intensity of the  $I_V^0$  line. Therefore, tensile strains observed are caused by different thermal expansion coefficients of ZnSe and GaAs. On the contrary, in the 200 nm ZnSe EL free exciton peak is not splitted and its spectral position is very close to the position of free exciton peak in bulk ZnSe (Fig. 3b). If one ascribes the peak observed to the  $X_{lh}$  component the value of tensile relative deformations in 200 nm ZnSe EL may be assumed to be less than  $0.03 \times 10^{-3}$ . This indicates low relaxation of the film at growth temperature and is proved by the absence of the  $I_V^0$  line in the emission spectrum.

As it follows from Fig. 3a, increase of Cd content in the QWs results in the low-energy shift of all ZnSe excitonic lines and in the increase of the energy difference between  $X_{hh}$  and  $X_{lh}$  peaks. It corresponds to the rise of tensile relative deformations from  $\varepsilon = 1.1 \times 10^{-3}$  for the QW with  $x = 0.23$  to  $\varepsilon = 2.8 \times 10^{-3}$  for the QW with  $x = 0.43$ . Recalculation of the spectral position of  $X_{hh}$  and  $X_{lh}$  peaks to the point  $\varepsilon = 0$  in the QW samples shows systematical shift of free exciton line position to the low-energy region (up to 3 meV for the QW sample with  $x = 0.43$ ) with the increase of Cd content in the QW. This testifies to the decrease of ZnSe cap layer band gap and can be due to Cd doping of ZnSe layers. Diffusion of Cd in ZnSe layers can also be the reason of the broadening of all excitonic lines and decrease of the  $I_V^0$  line intensity, which is very sensitive to the presence of impurities [12].

In contrast to the QW samples an apparent splitting of ZnSe free exciton peak is not observed in the QD structures (Fig. 3b). Thus we do not observe the changes in  $\varepsilon$  compared with 200 nm ZnSe EL. So, we can conclude that relative deformations in ZnSe layers of QD samples caused by ZnCdSe insert are significantly lower than in the case of the QW structures. However, ZnSe excitonic lines shift to the low-energy region and broaden with the increase of CdSe layer thickness (Fig. 3b). This testifies to significant interdiffusion processes in the QD samples.

It should be noted that in the PL spectra of the QD samples the  $I_V^0$  line arises in contrast to 200 nm ZnSe EL that indicates appearance of extended

defects. But the relative intensities of  $I_V^0$  line to free exciton line  $X$  in the QD structures is still significantly lower than that in the QW structures.

Fig. 4 shows the experimental  $(004)$   $\omega/2\theta$ -diffraction profiles for the QW and QD samples. On the low angle side of the intense substrate peak the signal from ZnSe layers is observed. For the QW samples weak signal from  $\text{Cd}_x\text{Zn}_{1-x}\text{Se}$  QW is also found. Diffraction profiles of the QW samples are modulated by interference caused by the phase shift induced by the  $\text{Cd}_x\text{Zn}_{1-x}\text{Se}$  layers [13]. However, the interference pattern is smeared that can be due to the nonuniform strain distribution and/or high defect concentration.

The measured  $\omega/2\theta$ -scans of the QD samples do not demonstrate any interference fringes.

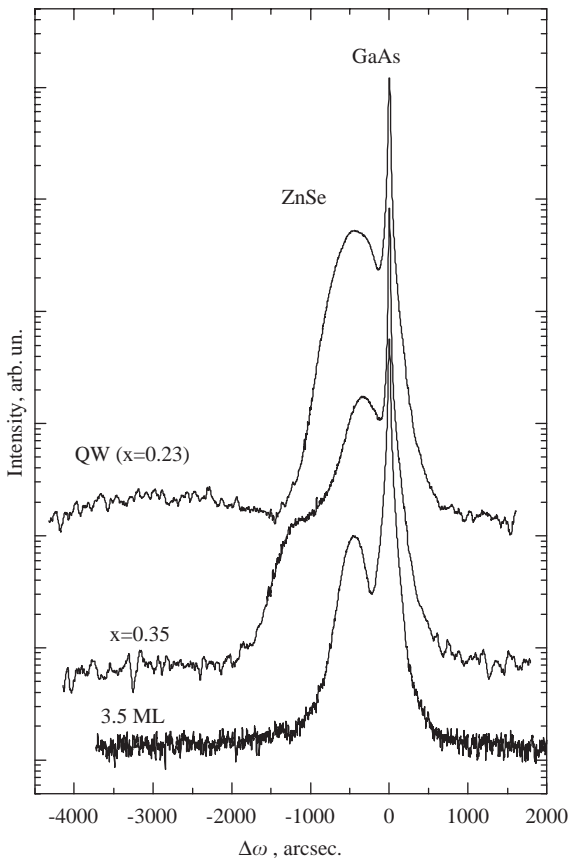


Fig. 4. Experimental  $(004)$   $\omega/2\theta$ -profiles of two  $\text{Cd}_x\text{Zn}_{1-x}\text{Se}/\text{ZnSe}$  QW heterostructures with  $x = 0.23$  and  $0.35$  and  $\text{CdSe}/\text{ZnSe}$  QD structure with  $3.5$  ML  $\text{CdSe}$  insert.

Disappearance of the interference pattern in the  $\text{CdSe}/\text{ZnSe}$  QD structures is usually explained by the increase of the extended defect density induced by large  $\text{CdZnSe}$  nanoislands with high Cd content [3,4]. This is in agreement with the PL data obtained.

The measured diffraction profiles were evaluated using simulations based on semi-kinematic diffraction theory [14]. From the position of the main ZnSe peak the values of strain in ZnSe layers were estimated. Evaluations show that  $1500$  nm ZnSe EL is under tensile strain of  $0.5 \times 10^{-3}$  in planar direction, while  $200$  nm ZnSe EL is under compressive strain of  $-1.4 \times 10^{-3}$  that confirms higher strain relaxation in former case. In the QW samples planar strains in ZnSe layers change with the increase of Cd content from compressive ( $-0.4 \times 10^{-3}$  in the sample with  $x = 0.23$ ) to tensile ones ( $0.06 \times 10^{-3}$  in the sample with  $x = 0.43$ ). In both the QD structures the ZnSe layers are found under compressive strain of  $-0.4 \times 10^{-3}$ .

#### 4. Discussion

The results of the PL investigations show that tensile deformation in the cap layer of the QW samples is several times greater than the value of  $\varepsilon$  in  $1500$  nm ZnSe EL and increases with the increase of Cd content in the QW. A rise of tensile additive to planar strains in ZnSe layers with the increase of Cd content in QW is confirmed also by X-ray diffraction measurements. However, in the latter case this additive ( $\sim 0.4 \times 10^{-3}$ ) is much lower than the one obtained from the PL spectrum analysis ( $\sim 1.5 \times 10^{-3}$ ).

The difference between the values of planar strains estimated from the PL spectra and X-ray diffraction profiles can be caused by several reasons. First of all, the temperatures of the PL measurements ( $T = 4.2$  K) and X-ray investigations ( $T = 300$  K) are different that results in the different lattice mismatch. Besides, in both methods different thickness of heterostructure is analysed. The PL spectra give the information about the strains averaged over the depth of the cap layer, while in the X-ray diffraction

measurements the whole heterostructure is analysed. In this case ZnSe buffer layer gives the main contribution in ZnSe signal in the diffraction profiles because of its higher thickness.

The results of the PL investigations of the QW structures have shown that increase of tensile strain in the cap layer is caused mainly by the influence of QW. Thus, analysis of the excitonic emission of ZnSe cap layer gives the possibility to obtain the information about the strain and its relaxation. This method was applied for strain control in the QD structures and showed that these structures are more relaxed compared with QW ones. This can be due to QD formation as well as due to the increase of extended defect density. The latter develops in appearance of the  $I_V^0$  line in spite of the evident interdiffusion processes that cause quenching of this line. However, extended defect density estimated from the relation of intensities of  $I_V^0$  line to  $X$  line in the QD structures is significantly lower than in the QW structures (Figs. 3a and b). Thus, strain relaxation observed in the QD structures cannot be caused by extended defect multiplication.

Analysis of the excitonic spectra of ZnSe cap layer in both QW and QD structures also shows the doping of cap layer by Cd. This develops in the low-energy shift and broadening of ZnSe excitonic lines as well as in decrease of  $I_V^0$  line intensity. In the QW structures a noticeable Cd/Zn interdiffusion is observed only when Cd content in QWs  $x \geq 35\%$ . Taking into account total quantity of Cd introduced we can conclude that in QD structures interdiffusion processes are more pronounced. This can be due to additional thermal annealing step used for QD formation. So, application of the growth methods that allows CdSe QD formation at lower temperature, for instance growth interruption [5], seems to be more suitable.

## 5. Conclusion

Investigations of strain relaxation processes in standard CdSe/ZnSe QW and QD heterostructures have been carried out by the photoluminescence and HRXRD methods.

It is shown that analysis of the excitonic spectra of ZnSe cap layer gives the information about strain and its relaxation in quantum-confinement structures, as well as about interdiffusion processes. In the cap layer of the QW structures with  $x = 0.2–0.4$  these deformations were estimated to be  $1–3 \times 10^{-3}$  and increased with the increase of Cd content in the QW. In the QD structures splitting of ZnSe free exciton line was not observed that indicated small value of strain. It is concluded that in spite of extended defect generation the main mechanism of strain relaxation in the QD structures is quantum dot formation. Significant doping of ZnSe cap layer with isovalent Cd impurity is found both in QW and QD structures. It is deduced that the method of CdSe QD formation using the growth interruption seems to be preferential compared with the method using thermal annealing step.

## Acknowledgements

One of the authors, L. Borkovska, was supported by the visiting grant Forschungsaufenthalte from German Academic Exchange Service (DAAD). She expresses her thanks to Dr. Michael Hoffmann and Andre Holzhey from the Institute of Applied Photophysics of the Technical University of Dresden for time-resolved PL experiments.

## References

- [1] S. Itoh, K. Nakano, A. Ishibashi, J. Crystal Growth 214/215 (2000) 1029.
- [2] M. Klude, T. Passow, R. Kroger, D. Hommel, Electron. Lett. 37 (2001) 1119.
- [3] T. Passow, K. Leonardi, A. Stockmann, H. Selke, H. Heinke, D. Hommel, J. Phys. D.: Appl. Phys. 32 (1999) A42.
- [4] D. Litvinov, D. Grethsen, A. Rosenauer, H. Preis, E. Kurtz, C. Klingshirn, Phys. Stat. Sol. (b) 224 (2001) 147.
- [5] F. Gindele, U. Woggon, W. Langbein, J.M. Hvam, K. Leonardi, D. Hommel, H. Selke, Phys. Rev. B 60 (1999) 8773.
- [6] E. Kurtz, J. Shen, M. Schmidt, M. Grun, S.K. Hong, D. Litvinov, D. Gerthsen, T. Oka, T. Yao, C. Klingshirn, Thin Solid Films 367 (2000) 68.

- [7] M. Godlewski, J.P. Bergman, B. Monemar, E. Kurtz, D. Hommel, *J. Crystal Growth* 159 (1996) 533.
- [8] R. Cingolani, P. Prete, D. Greco, P.V. Giugno, M. Lomascolo, R. Rinaldi, C. Calcagnile, L. Vanzetti, L. Sorba, A. Franciosi, *Phys. Rev. B* 51 (1994) 5176.
- [9] N. Peranio, A. Rosenauer, D. Gerthsen, S.V. Sorokin, I.V. Sedova, S.V. Ivanov, *Phys. Rev. B* 61 (2000) 16015.
- [10] S. Wachter, B. Dal Don, M. Schmidt, M. Baldauf, A. Dinger, E. Kurtz, C. Klingshirn, H. Kalt, *Phys. Stat. Sol (b)* 224 (2001) 437.
- [11] J. Gutowski, N. Presser, G. Kudlek, *Phys. Stat. Sol. (a)* 120 (1990) 11.
- [12] K. Shahzad, J. Petruzzello, D.J. Olego, D.A. Cammack, *Appl. Phys. Lett.* 57 (1990) 2452.
- [13] T. Passow, H. Heinke, J. Falta, K. Leonardi, D. Hommel, *Appl. Phys. Lett.* 77/22 (2000) 3544.
- [14] V. Holy, U. Pietch, T. Baumbach, *High-Resolution X-ray Scattering from Thin Films and Multilayers*, Springer, Berlin, 1998, p. 254.